UNIABUJA Journal of Engineering and Technology

https://ujet.uniabuja.edu.ng/

ISSN: 2714-3236 (Online); 2714-3228 (Print)

Volume 3, Issue 1, 2026; 168-181

Scheffe's Optimization of the Compressive and Flexural Strengths of a Self-Compacting Laterite Concrete

Emmanuel E. NDUBUBA[1], Daniel O. OJILE[2*], Muoka ANTHONY[3], Innocent T. NTEYOHO[4]

[1,2,3,4]*Department of Civil Engineering, University of Abuja, Abuja, Nigeria*

[1]*emmanuel.ndububa@uniabuja.edu.ng*, [2*]*danielojile06@gmail.com*, [3]*anthony.muoka@nileuniversity.edu.ng*, [4]*nteyohoinnocent@gmail.com*

Abstract

This research investigates the use of laterite as a partial replacement for fine aggregate in self-compacting concrete (SCC) with the aim of enhancing sustainability, reducing material cost, and promoting the utilization of locally available materials. A total of 56 concrete mix proportions were developed using Scheffé's simplex lattice design method N(6,3) to systematically assess the effects of varying laterite contents on compressive strength, flexural strength, and workability. Hydroplast 260GR, a high-range water-reducing admixture, was incorporated at dosages of up to 2.0% by weight of cement to achieve adequate flowability while minimizing water demand. The compressive strength of the SCC mixes ranged from 12.90 MPa to 22.70 MPa, while flexural strength values varied between 2.42 MPa and 3.22 MPa. Results revealed a general reduction in strength with increasing laterite content, particularly at higher replacement levels. However, several optimized mixes satisfied the minimum strength requirements for structural concrete. Slump flow values ranged between 550 mm and 590 mm, meeting EFNARC specifications for SCC. Regression models developed for compressive and flexural strengths demonstrated strong predictive capability, with coefficients of determination (R^2) exceeding 97%. Analysis of variance (ANOVA) confirmed the statistical significance of the models. Optimization results indicated that an SCC mix containing approximately 4.95% laterite by volume of fine aggregate achieved a compressive strength of 21.67 MPa and a flexural strength of 3.13 MPa, with a corresponding 3.5% reduction in production cost. The findings confirm that laterite can be effectively utilized in SCC for sustainable construction applications.

Keywords: *Laterite, Optimization, Concrete, Self-Compacting Concrete.*

1.0 Introduction.

Concrete is one of the most widely used construction materials owing to its durability, strength, and versatility. It is composed of several primary constituents, including cement, aggregates, water, and additives [1]. The aggregates, which mostly account for 60-80% of the concrete volume, play a significant role in determining its mechanical properties, and the two main types of aggregates used in concrete are coarse aggregates and fine aggregates [2]. Coarse aggregates, which include crushed stone or gravel, provide bulk and stability to the concrete mixture, while fine aggregates, mostly in the form of sand, fill the gaps between the coarse particles, thereby improving workability and contributing to the overall strength of the concrete [3]. Self-compacting concrete (SCC) is a pioneering concrete that does not require vibration for placement and compaction. It is able to flow under its own weight, completely filling formwork and achieving full compaction, even in the presence of congested reinforcement. SCC is a high-performance concrete that consolidates under its self-weight and adequately fills all voids without segregation, excessive bleeding, or any other separation of materials, without the need for mechanical consolidation. The key properties of SCC are filling ability, passing ability, and resistance to segregation. Filling ability enables SCC to flow through the formwork and completely fill all spaces within it. Passing ability is the property by which it flows without blocking. The benefit of resistance to segregation imparts the advantage to the concrete in maintaining a uniform composition, hence the paste and the aggregate bind together [4]. Present-day self-compacting concrete can be classified as an advanced construction material. As the name suggests, it does not require vibration to achieve full compaction. This offers many benefits and advantages over conventional concrete, including improved quality of concrete, reduction of on-site repairs, faster construction times, lower overall costs, facilitation of automation in concrete construction, high performance, improved durability, and high strength. An important improvement in health and safety is also achieved through the elimination of vibrator handling and a substantial reduction in environmental noise loading on and around a site. The composition of SCC mixes includes substantial proportions of fine-grained inorganic materials, providing possibilities for the utilization of mineral admixtures, which are currently waste products with no practical applications. For SCC, it is generally important to use superplasticizers to obtain high mobility [5]. Self-compacting concrete

Received: 20-10-2026 / Accepted: 15-12-2025 / Published: 02-02-2026

https://doi.org/10.70118/ujet.2026.0301.16

has been successfully used in Japan, Denmark, France, the U.K., and other countries [4]. Cement, another critical component of concrete, acts as a binding agent that holds the aggregates together. It undergoes a chemical reaction known as hydration, where it reacts with water to form a solid matrix that binds the aggregates into a cohesive mass [2]. The quality and type of cement used can significantly influence the strength and durability of the concrete. Water is essential in the concrete mixture for the hydration process to occur. The water-to-cement ratio plays a critical role in achieving the desired workability and strength. Excess water can weaken the concrete and lead to increased porosity, while insufficient water can hinder the hydration process and result in poor strength development [6]. Additives, such as admixtures, are often incorporated into the concrete mixture to modify its properties. These admixtures improve workability, speed up or slow down the hydration process, enhance durability, or provide other specific functions based on the desired concrete characteristics. Understanding the properties and interactions of these constituents is key to designing and producing concrete with optimal strength, durability, and workability. The composition, proportioning, and processing of these constituents can be adjusted to meet specific project requirements and environmental conditions [2]. The selection of suitable aggregates significantly impacts the strength and performance of concrete. While traditional fine aggregates like river sand are commonly used, alternative materials such as laterite have gained attention in recent times. Laterite, a soil-like material rich in iron and aluminum oxides, is found abundantly in tropical and subtropical regions. Utilizing laterite as a fine aggregate in concrete offers potential for sustainable construction practices, cost reduction, and reduced environmental impact [7]. Lateritic soils are highly weathered and altered residual soils formed by the in-situ weathering and decomposition of parent rocks under tropical and subtropical climatic conditions [8]. This weathering process mainly involves the continuous chemical alteration of minerals, the release of iron and aluminum oxides, and the removal of bases and silica in the rocks. Lateritic soils are void or nearly void of bases, mainly silicates, but may contain substantial amounts of quartz and kaolinite [9]. They are formed in hot, wet tropical regions with an annual rainfall of at least 1200 mm and a daily temperature exceeding 25°C, typically occurring in humid tropical climates within 30°N and 30°S of the equator. Laterite is composed entirely of iron and aluminum oxide, reddish in color, and is the least soluble product of rock weathering in tropical climates [10]. Lateritic soil is one of the most common and important materials used in earthwork engineering construction in the tropics and subtropics where it is abundant. Compressive strength is a fundamental mechanical property of concrete that measures its ability to resist axial loading and plays a vital role in ensuring the structural integrity of concrete elements such as columns, walls, and foundations [11]. The compressive strength indicates the maximum compressive stress that the concrete can withstand without failure. It is essential for determining the load-carrying capacity of structures and preventing collapse or deformation [12].

Higher compressive strength allows the concrete to bear heavier loads and ensures the long-term stability and safety of structures. Furthermore, compressive strength is closely related to the durability of concrete, as higher compressive strength generally indicates better resistance to environmental factors such as freeze-thaw cycles, chemical attack, and abrasion. It helps prevent cracking, spalling, and deterioration, thereby ensuring the longevity and performance of the concrete in challenging conditions [13]. Flexural strength, also known as the modulus of rupture, evaluates the ability of concrete to resist bending or flexural stresses and is especially crucial for structural elements subjected to bending, such as beams and slabs [14]. The flexural strength indicates the maximum tensile stress that the concrete can withstand before it fractures [15]. Adequate flexural strength is essential for ensuring that structures can safely carry imposed loads and retain their intended shapes and functions. It enables concrete elements to withstand bending without fracturing, providing necessary structural support [2]. Both compressive and flexural strengths are essential parameters in structural design. Engineers utilize these strengths to calculate the required dimensions, reinforcement, and load-bearing capacities of concrete elements. Understanding compressive and flexural strengths allows designers to ensure that concrete structures meet necessary safety and performance criteria. By considering these strengths, designers can optimize the dimensions and reinforcement of elements, ensuring their ability to withstand expected loads and maintain structural integrity over time [16].

2.0 Materials and Methods

2.1 Materials

The fine aggregate used was natural river sand obtained from Jere Sand, Abuja. It was characterized by smooth and rounded particles. Laterite, sourced from a borrow pit at Jahi, FCT Abuja, was reddish-brown in color, fine-grained in texture, and observed to harden during the dry season. The coarse aggregate was procured from Zeberceed Quarry in Kubwa, FCT Abuja. Potable borehole water suitable for domestic consumption was used for mixing and curing throughout the experimental program. Water played a critical role in initiating the hydration process of cement and other constituents, and its quantity was carefully regulated to assess its effect on the workability and strength of the self-compacting concrete (SCC). A chemical admixture, Hydroplast 260GR superplasticizer, was incorporated to enhance the workability of the concrete

Received: 20-10-2026 / Accepted: 15-12-2025 / Published: 02-02-2026

https://doi.org/10.70118/ujet.2026.0301.16

while reducing water demand. Its dosage, optimized through preliminary trials, did not exceed 2.0% by weight of cement. Hydroplast 260GR is a high-range water-reducing admixture designed to produce high-slump concrete with superior workability retention. The key properties of the admixture are presented in Table 1.

Table 1: Properties of Hydroplast 260GR

SN	Colour	Brown
1	Density	1.16g/cm^3
2	Chloride content	"Chloride-free" to EN 934
3	Freezing point	0°C
4	PH	7-9

2.2 Methods

The sedimentation test was conducted to determine the particle size distribution of laterite soil by measuring the rate of particle settlement in water, in accordance with BS 1377-2:1990 [22]. The test apparatus comprised a graduated sedimentation cylinder, distilled water, a dispersing agent, mixing tools, a metric scale, and a timer. The oxide composition of the laterite was determined using X-ray fluorescence (XRF) spectroscopy, which is a standardized technique for elemental and oxide analysis of geomaterials [23]. The analysis identified major oxides including SiO_2, Al_2O_3, Fe_2O_3, CaO, MgO, K_2O, and Na_2O. The combined percentage of SiO_2, Al_2O_3, and Fe_2O_3 satisfied established pozzolanic criteria, confirming the suitability of laterite for use in self-compacting concrete (SCC) [24]. Steel cube moulds measuring 150 mm × 150 mm × 150 mm (0.003375 m^3) were used for casting concrete specimens. Mix proportions were developed using Scheffé's simplex lattice mixture design method, which is widely applied for concrete optimization involving multiple constituents [25]. For a six-component, third-degree simplex lattice, the minimum number of experimental mixes was calculated as 56, with three replicate specimens produced per mix, resulting in a total of 168 samples. The fresh properties of SCC were evaluated using the slump flow test, conducted in accordance with BS EN 12350-8:2010 and ASTM C143/C143M [26], [27]. Compressive strength tests were performed on cube specimens in line with BS EN 12390-2:2000 and BS 1881-116:1983 [28], [29]. Specimens were demoulded after 24 hours, cured in water, and tested at 28 days using a digital compression testing machine. Flexural strength was determined following BS EN 12390-5:2009, using centrally loaded prism specimens [30]. Statistical optimization of mix proportions was carried out using Response Surface Methodology (RSM) supported by Analysis of Variance (ANOVA) to evaluate the significance of mix variables and model adequacy [31]. Scheffé's mixture design algorithm was also employed, with water, cement, fine aggregate, laterite, superplasticizer, and coarse aggregate represented as pseudo-components X_1 to X_6. This combined approach ensured the development of optimized SCC mixtures that balanced mechanical strength and workability.

Table 2: Mix proportions

Density (kg/cum) = Samples	Water	Cement	Fine Agg	Laterite	Super plast	Coarse Agg
	1000	1440	1711	1883	1160	2152
	A1	A2	A3	A4	A5	A6
S1	0.513	0.932	2.436	0.000	0.014	2.785
S2	0.513	0.932	2.38	0.061	0.015	2.785
S3	0.513	0.932	2.324	0.122	0.016	2.784
S4	0.512	0.931	2.269	0.183	0.017	2.784
S5	0.512	0.931	2.213	0.244	0.018	2.783
S6	0.512	0.931	2.157	0.304	0.019	2.783
S7	0.513	0.932	2.408	0.03	0.014	2.785
S8	0.513	0.932	2.38	0.061	0.015	2.785
S9	0.513	0.932	2.352	0.091	0.015	2.785
S10	0.513	0.932	2.324	0.122	0.016	2.784
S11	0.512	0.931	2.297	0.152	0.016	2.784
S12	0.513	0.932	2.352	0.091	0.015	2.785
S13	0.513	0.932	2.324	0.122	0.016	2.784

Received: 20-10-2026 / Accepted: 15-12-2025 / Published: 02-02-2026

https://doi.org/10.70118/ujet.2026.0301.16

S14	0.512	0.931	2.297	0.152	0.016	2.784
S15	0.512	0.931	2.269	0.183	0.017	2.784
S16	0.512	0.931	2.297	0.152	0.016	2.784
S17	0.512	0.931	2.269	0.183	0.017	2.784
S18	0.512	0.931	2.241	0.213	0.017	2.784
S19	0.512	0.931	2.241	0.213	0.017	2.784
S20	0.512	0.931	2.213	0.244	0.018	2.783
S21	0.512	0.931	2.185	0.274	0.018	2.783
S22	0.507	0.932	2.38	0.061	0.015	2.785
S23	0.507	0.932	2.362	0.081	0.015	2.785
S24	0.507	0.932	2.343	0.102	0.015	2.785
S25	0.507	0.932	2.324	0.122	0.016	2.784
S26	0.507	0.932	2.343	0.102	0.015	2.785
S27	0.507	0.932	2.324	0.122	0.016	2.784
S28	0.507	0.932	2.306	0.142	0.016	2.784
S29	0.507	0.932	2.306	0.142	0.016	2.784
S30	0.507	0.931	2.287	0.162	0.016	2.784
S31	0.507	0.931	2.269	0.183	0.017	2.784
S32	0.507	0.932	2.324	0.122	0.016	2.784
S33	0.507	0.932	2.306	0.142	0.016	2.784
S34	0.507	0.931	2.287	0.162	0.016	2.784
S35	0.507	0.931	2.287	0.162	0.016	2.784
S36	0.507	0.931	2.269	0.183	0.017	2.784
S37	0.507	0.931	2.250	0.203	0.017	2.784
S38	0.507	0.932	2.417	0.02	0.014	2.785
S39	0.507	0.932	2.399	0.041	0.014	2.785
S40	0.507	0.932	2.380	0.061	0.015	2.785
S41	0.507	0.932	2.362	0.081	0.015	2.785
S42	0.507	0.932	2.343	0.102	0.015	2.785
S43	0.507	0.932	2.399	0.041	0.014	2.785
S44	0.507	0.932	2.362	0.081	0.015	2.785
S45	0.507	0.932	2.343	0.102	0.015	2.785
S46	0.507	0.932	2.324	0.122	0.016	2.784
S47	0.507	0.932	2.306	0.142	0.016	2.784
S48	0.507	0.932	2.362	0.081	0.015	2.785
S49	0.507	0.932	2.343	0.102	0.015	2.785
S50	0.507	0.932	2.306	0.142	0.016	2.784
S51	0.507	0.931	2.287	0.162	0.016	2.784
S52	0.507	0.931	2.269	0.183	0.017	2.784
S53	0.507	0.932	2.324	0.122	0.016	2.784
S54	0.507	0.932	2.306	0.142	0.016	2.784
S55	0.507	0.931	2.287	0.162	0.016	2.784
S56	0.507	0.931	2.250	0.203	0.017	2.784
TOTAL	28.514	52.170	129.564	7.482	0.891	155.920

Received: 20-10-2026 / Accepted: 15-12-2025 / Published: 02-02-2026

https://doi.org/10.70118/ujet.2026.0301.16

3.0 Results and Discussion

3.1 Laterite Properties

The chemical composition of the laterite revealed that silicon dioxide (SiO_2) was the dominant oxide, constituting slightly over 32% of the total composition, indicating a predominantly sandy and quartz-rich material. High silica content in lateritic soils has been widely associated with improved particle interlock and strength development when used in cementitious composites [17], [32]. Sedimentation analysis further classified the material as sandy clay under the Unified Soil Classification System (USCS), comprising approximately 67% sand, 21.3% clay, and 11.2% silt (Table 3). Such grading has been reported to promote favorable particle packing and mechanical performance in concrete, although increased sand content may marginally reduce plasticity and fresh concrete workability [33], [34]. Aluminum oxide (Al_2O_3), accounting for approximately 20%, confirmed the presence of alumina-bearing minerals such as gibbsite and kaolinite, which are typical constituents of lateritic soils formed under tropical weathering conditions [35]. Iron (III) oxide (Fe_2O_3), present at about 8%, was responsible for the characteristic reddish coloration of the laterite and has been shown to contribute to enhanced particle bonding and hardness in laterized concrete systems [36]. Minor oxides such as magnesium oxide (MgO, ~6%) were indicative of basic mineral phases that enhance chemical stability, while trace amounts of titanium dioxide (TiO_2) are commonly reported in tropical residual soils and do not adversely affect concrete performance [37]. The contents of phosphorus pentoxide (P_2O_5) and sulfur trioxide (SO_3) were negligible, which is desirable for concrete durability, as excessive sulfates and phosphates are known to cause expansion, cracking, and long-term deterioration in cement-based materials [38], [39]. Overall, the predominance of SiO_2, Al_2O_3, and Fe_2O_3, combined with the absence of deleterious oxides, confirms that the laterite used in this study (Figure 1) possesses favorable mineralogical characteristics for civil engineering applications, particularly as a sustainable fine aggregate replacement in self-compacting concrete. Regional characterization studies of Abuja laterites similarly report silica- and alumina-dominated compositions, further supporting the suitability of lateritic materials for concrete production in tropical environments [17], [40].

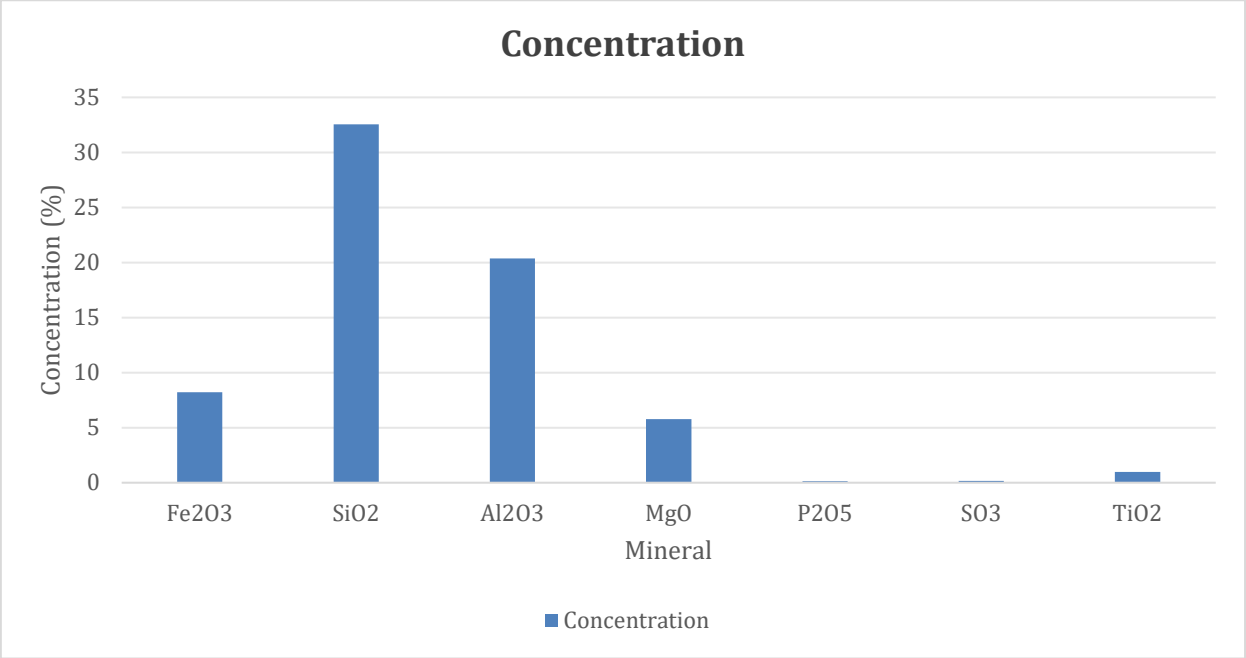

Figure 1: Laterite percentage mineral composition

Table 3: Laterite Sedimentation Test Analysis

S/N	Soil Fraction	Percentage (%)
1	Sand	67.0
2	Silt	11.2
3	Clay	21.3

3.2 Effect of Laterite on the workability of SCC

Self-compacting concrete is designed to flow under its own weight and fill formwork without the need for mechanical vibration. A key requirement for SCC is high flowability, typically assessed using slump flow tests. The incorporation of Hydroplast 260GR, a high-range water-reducing admixture, enhanced paste fluidity and maintained a low water-to-cement ratio while ensuring adequate flowability. The slump-flow

Received: 20-10-2026 / Accepted: 15-12-2025 / Published: 02-02-2026

https://doi.org/10.70118/ujet.2026.0301.16

values (550–590 mm) satisfied EFNARC (2005) criteria for self-compacting concrete. Although laterite addition increased the fine fraction, its effect on flow was minimal due to the dispersing efficiency of the superplasticizer, which reduced inter-particle friction. Mixes with up to 3.66% laterite exhibited stable flow characteristics, indicating that optimized admixture dosage effectively mitigates the higher water demand of lateritic fines. Minor reductions in flow at higher laterite levels were attributed to surface absorption and reduced paste availability. These results confirm that laterized SCC preserves self-compacting performance when superplasticizer dosage is properly optimized as shown in figure 2. Previous studies have shown that the particle size distribution and fines content of laterite strongly influence fresh and hardened concrete properties, reinforcing the need for admixture optimization when laterite is used as a partial sand replacement [18].

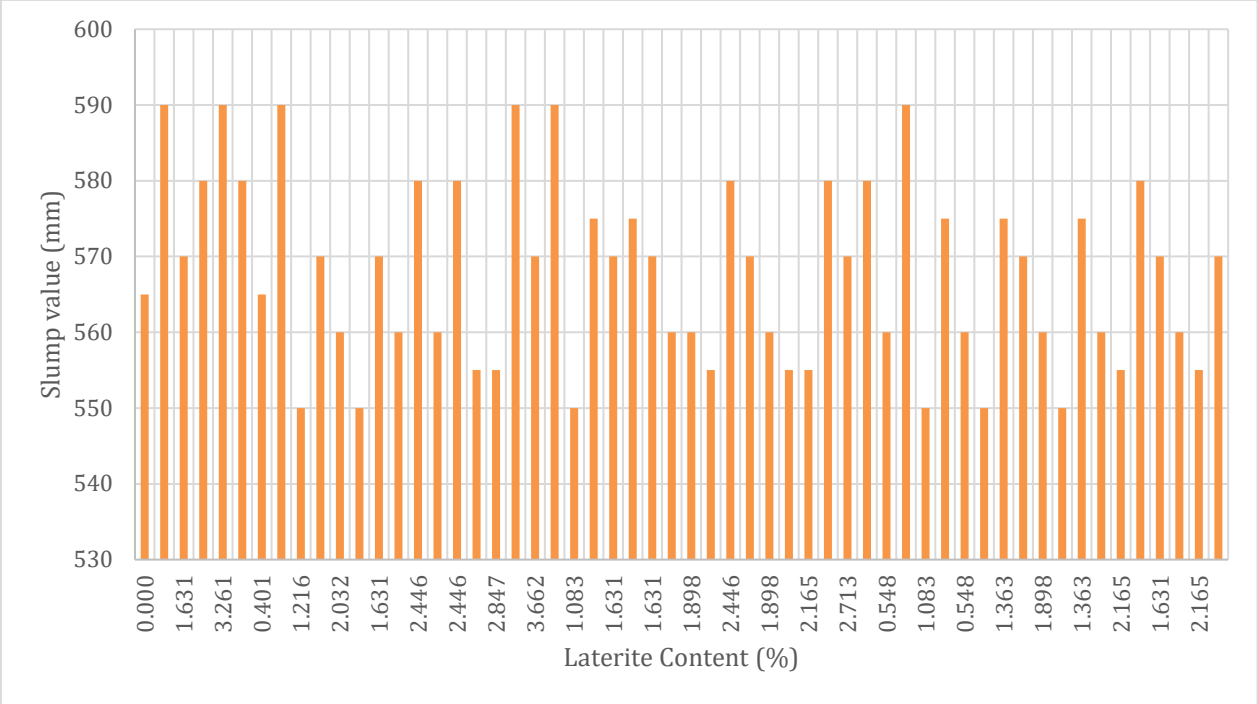

Figure 2: Relationship between laterite content and slump value of SCC

The workability performance indicates that laterite incorporation can enhance the sustainability of self-compacting concrete (SCC) by partially substituting natural fine aggregates without compromising fresh-state properties. However, due to the sensitivity of SCC to variations in fine content and moisture demand, laterite addition must be carefully controlled to avoid segregation or bleeding. The consistent slump-flow values observed across varying laterite proportions demonstrate good mix stability, a critical attribute for maintaining homogeneity during placement. As shown in Figure 2, most mixes achieved flow values within the EFNARC-specified range, confirming the material's suitability as a partial fine aggregate. Although some mixes approached the lower flow threshold, the overall results suggest that minor adjustments in paste volume or superplasticizer dosage can fully restore optimal flowability. These findings affirm that laterite-modified SCC can achieve the desired balance of workability and stability, providing a sustainable and locally viable alternative for concrete production in regions where laterite is abundant.

3.3 Laterite and SCC Compressive Strength and Flexural Strength

The results presented in Figures 3 and 4 reveal a general decline in both compressive and flexural strengths with increasing laterite content, as indicated by the red trendline. At low replacement levels (<1.5%), compressive strengths remained relatively high, often exceeding 18 MPa and, in some cases, reaching 20 MPa. Beyond this threshold, a marked reduction was observed, with values clustering between 13 and 17 MPa, particularly within the 2–3.5% laterite range. A similar trend occurred in flexural strength, which decreased from approximately 3.0 MPa at 0% laterite to 2.5 MPa at 4%.

This strength reduction is primarily attributed to the high fines content and porous, irregular particle morphology of laterite, which increase water demand and weaken the interfacial transition zone (ITZ) between the paste and aggregates. In SCC, where homogeneity and cohesion are critical, such microstructural irregularities can disrupt stress transfer and reduce mechanical performance. Excessive fines also hinder aggregate interlock, further contributing to the decline in strength. Nonetheless, isolated data points at higher laterite contents showing improved strength suggest that optimized mix design parameters—such as controlled water-to-binder ratio, proper superplasticizer dosing, and blending with well-graded sand—can

Received: 20-10-2026 / Accepted: 15-12-2025 / Published: 02-02-2026

https://doi.org/10.70118/ujet.2026.0301.16

mitigate these effects. Overall, the findings indicate that laterite replacement up to about 1.5% can be safely adopted in SCC without significant loss of strength, while higher proportions require careful mix optimization to preserve structural integrity.

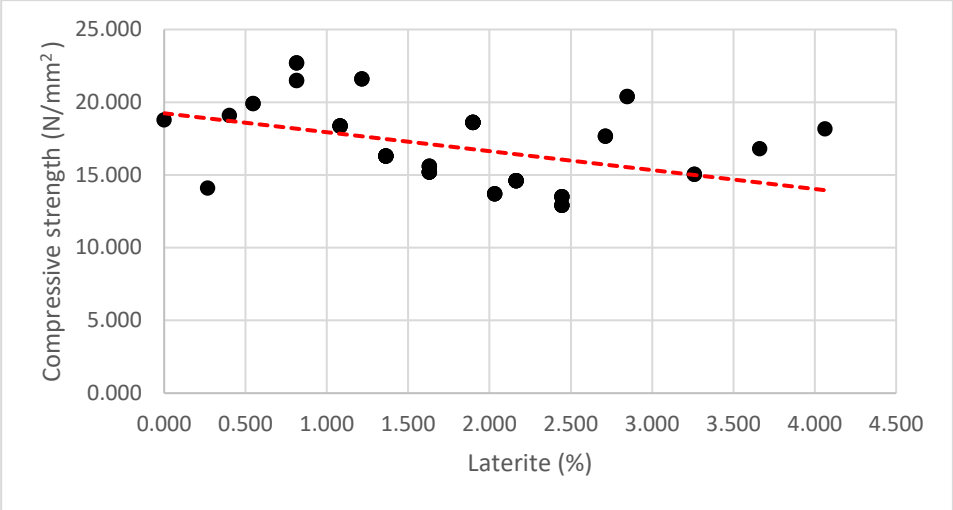

Figure 3: Laterite content vs SCC Compressive strength

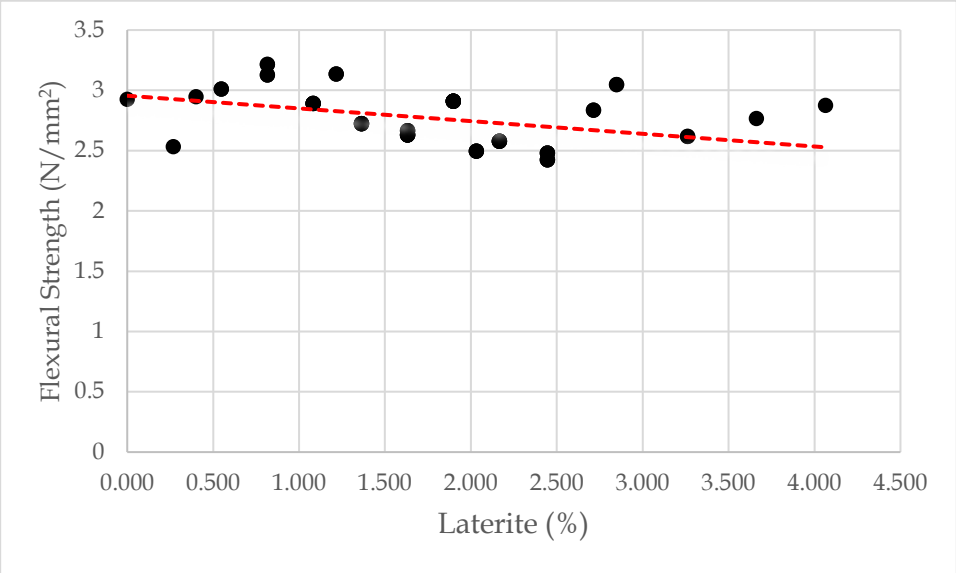

Figure 4: Laterite content vs SCC Flexural strength

3.4 Compressive and Flexural Strength Model and Responses

Table 4 presents the 28-day compressive strength results of the self-compacting laterite concrete (SCLC) mixes developed using Scheffé's simplex lattice design. The results indicate that compressive strength varies significantly with changes in mix proportions, particularly the laterite replacement level and cement content. Mixes with lower laterite content generally exhibited higher compressive strength, which can be attributed to the reduced presence of fine lateritic particles that tend to increase water demand and weaken the cement–aggregate bond when used excessively. The compressive strength values ranged between the minimum and maximum limits specified for structural concrete, demonstrating that laterite can be effectively incorporated into SCC without compromising strength when properly proportioned. The observed trend confirms that while laterite contributes to improved particle packing at low replacement levels, excessive laterite content leads to strength reduction due to its relatively higher clay fraction and lower stiffness compared to natural sand. The consistency of results across replicate specimens also indicates good experimental reliability and uniformity of mixing and curing conditions. Compressive strength values across the SCC samples varied significantly, ranging from as low as 12.90 MPa (Z156 and Z336) to as high as 22.70 MPa (Z2, Z13, Z114) as shown in table 4. The high-strength mixes typically contained little or no laterite, or had balanced ternary blends. Notably, mixes like Z2 and Z13, which yielded the highest mean compressive strength of 22.70 MPa,

Received: 20-10-2026 / Accepted: 15-12-2025 / Published: 02-02-2026

https://doi.org/10.70118/ujet.2026.0301.16

consisted of optimal fine aggregate and cement ratios with minimal interaction effects from laterite. The regression analysis as shown in table 5 further clarified this observation: many interaction terms involving laterite (e.g., β15, β16, β25, β26) had significantly negative coefficients (e.g., β16 = -6.995, $p < 0.001$), demonstrating a statistically significant weakening effect of excessive laterite on compressive strength. Positive interaction terms (e.g., β13 = 5.305, β34 = 2.505) suggest that synergistic combinations involving traditional aggregates contribute positively to strength. Flexural strength results mirrored the compressive strength trend, with values ranging from 2.42 MPa (Z156, Z336) to 3.22 MPa (Z2, Z13) as shown in table 4. The highest flexural strengths were found in mixes with optimized cement-to-fine aggregate ratios and minimal or well-balanced laterite proportions. Overall, Table 4 confirms that optimized SCLC mixes can achieve satisfactory compressive strength suitable for structural applications, provided that laterite replacement is carefully controlled. Table 5 summarizes the 28-day flexural strength results of the SCLC mixes. Flexural strength followed a trend similar to compressive strength, with higher values recorded for mixes containing lower to moderate laterite content. This behavior reflects the sensitivity of flexural performance to aggregate grading, paste quality, and interfacial bond strength within the concrete matrix. The results indicate that flexural strength decreases gradually as laterite content increases beyond the optimal range. This reduction is primarily attributed to the increased fine content and clay minerals present in laterite, which may weaken the interfacial transition zone and reduce resistance to tensile stresses. Nevertheless, several mixes achieved flexural strength values comparable to those of conventional SCC, demonstrating that laterite can be used without significant loss of performance when properly optimized. The flexural strength results presented in Table 5 further validate the regression and optimization models developed in this study, as the experimental values closely align with predicted outcomes. These findings support the suitability of laterite-based SCC for applications where moderate flexural performance is required, such as slabs, pavements, and precast elements. Flexural performance as shown in table 5 was most adversely affected by higher-order interaction terms involving laterite, as reflected in coefficients like β156 = -0.672 and β245 = -0.468, all with p-values < 0.001. These suggest that tripartite interactions including laterite introduce microstructural inconsistencies, potentially due to its high surface area, absorption capacity, and irregular particle morphology.

Table 4: Results of Sample Response to Scheffe's N(6, 3) Water, Cement, Fine-Aggregate, Laterite Soil, Coarse Aggregate, and Superplasticizer

S/N	Points	Compressive Strength(N/mm2)				Flexural Strength(N/mm2)				Slump Value
	0	Trial -1	Trial -2	Trial -3	Mean	Trial -1	Trial -2	Trial -3	Mean	
1	Z1	18.37	20.70	17.30	18.79	2.89	3.07	2.81	2.93	565.00
2	Z2	24.30	22.70	21.10	22.70	3.23	3.22	3.21	3.22	590.00
3	Z3	13.60	15.50	17.70	15.60	2.50	2.66	2.84	2.67	570.00
4	Z4	13.20	14.70	12.60	13.50	2.45	2.59	2.40	2.48	580.00
5	Z5	16.30	14.15	14.70	15.05	2.73	2.54	2.59	2.62	590.00
6	Z6	18.51	17.31	18.70	18.17	2.90	2.81	2.92	2.88	580.00
7	Z12	18.60	17.90	20.80	19.10	2.91	2.86	3.08	2.95	565.00
8	Z13	24.30	22.70	21.10	22.70	3.23	3.22	3.21	3.22	590.00
9	Z14	20.80	22.40	21.60	21.60	3.08	3.20	3.14	3.14	550.00
10	Z15	13.60	15.50	17.70	15.60	2.50	2.66	2.84	2.67	570.00
11	Z16	12.40	13.60	15.10	13.70	2.38	2.49	2.63	2.50	560.00
12	Z23	20.80	22.40	21.60	21.60	3.08	3.20	3.14	3.14	550.00
13	Z24	13.60	15.50	17.70	15.60	2.50	2.66	2.84	2.67	570.00
14	Z25	12.40	13.60	15.10	13.70	2.38	2.49	2.63	2.50	560.00
15	Z26	13.20	14.70	12.60	13.50	2.45	2.59	2.40	2.48	580.00
16	Z34	12.40	13.60	15.10	13.70	2.38	2.49	2.63	2.50	560.00
17	Z35	13.20	14.70	12.60	13.50	2.45	2.59	2.40	2.48	580.00
18	Z36	19.40	21.20	20.60	20.40	2.97	3.06	3.11	3.05	555.00
19	Z45	19.40	21.20	20.60	20.40	2.97	3.06	3.11	3.05	555.00
20	Z46	16.30	14.15	14.70	15.05	2.73	2.54	2.59	2.62	590.00
21	Z56	18.20	15.80	16.40	16.80	2.88	2.68	2.74	2.77	570.00
22	Z123	21.50	20.70	22.30	21.50	3.13	3.07	3.19	3.13	590.00
23	Z124	18.90	17.50	18.70	18.37	2.94	2.82	2.92	2.89	550.00
24	Z125	16.50	14.80	17.60	16.30	2.74	2.83	2.60	2.73	575.00
25	Z126	15.80	15.90	13.80	15.20	2.68	2.51	2.71	2.63	570.00
26	Z134	16.50	14.80	17.60	16.30	2.74	2.83	2.60	2.73	575.00
27	Z135	15.80	15.90	13.80	15.20	2.68	2.51	2.71	2.63	570.00

Received: 20-10-2026 / Accepted: 15-12-2025 / Published: 02-02-2026

https://doi.org/10.70118/ujet.2026.0301.16

S/N	Points	Compressive Strength(N/mm2)				Flexural Strength(N/mm2)				Slump Value
	0	Trial -1	Trial -2	Trial -3	Mean	Trial -1	Trial -2	Trial -3	Mean	
28	Z136	19.90	17.40	18.50	18.60	3.01	2.82	2.91	2.91	560.00
29	Z145	19.90	17.40	18.50	18.60	3.01	2.82	2.91	2.91	560.00
30	Z146	13.70	15.90	14.20	14.60	2.50	2.69	2.55	2.58	555.00
31	Z156	11.70	14.20	12.80	12.90	2.31	2.54	2.42	2.42	580.00
32	Z234	15.80	15.90	13.80	15.20	2.68	2.51	2.71	2.63	570.00
33	Z235	19.90	17.40	18.50	18.60	3.01	2.82	2.91	2.91	560.00
34	Z236	13.70	15.90	14.20	14.60	2.50	2.69	2.55	2.58	555.00
35	Z245	13.70	15.90	14.20	14.60	2.50	2.69	2.55	2.58	555.00
36	Z246	11.70	14.20	12.80	12.90	2.31	2.54	2.42	2.42	580.00
37	Z256	18.60	17.51	16.90	17.67	2.91	2.83	2.78	2.84	570.00
38	Z112	12.50	14.60	15.20	14.10	2.39	2.58	2.64	2.53	580.00
39	Z113	19.50	19.00	21.20	19.90	2.98	2.94	3.11	3.01	560.00
40	Z114	21.50	20.70	22.30	21.50	3.13	3.07	3.19	3.13	590.00
41	Z115	18.90	17.50	18.70	18.37	2.94	2.82	2.92	2.89	550.00
42	Z116	16.50	14.80	17.60	16.30	2.74	2.83	2.60	2.73	575.00
43	Z221	19.50	19.00	21.20	19.90	2.98	2.94	3.11	3.01	560.00
44	Z223	18.90	17.50	18.70	18.37	2.94	2.82	2.92	2.89	550.00
45	Z224	16.50	14.80	17.60	16.30	2.74	2.83	2.60	2.73	575.00
46	Z225	15.80	15.90	13.80	15.20	2.68	2.51	2.71	2.63	570.00
47	Z226	19.90	17.40	18.50	18.60	3.01	2.82	2.91	2.91	560.00
48	Z331	18.90	17.50	18.70	18.37	2.94	2.82	2.92	2.89	550.00
49	Z332	16.50	14.80	17.60	16.30	2.74	2.83	2.60	2.73	575.00
50	Z334	19.90	17.40	18.50	18.60	3.01	2.82	2.91	2.91	560.00
51	Z335	13.70	15.90	14.20	14.60	2.50	2.69	2.55	2.58	555.00
52	Z336	11.70	14.20	12.80	12.90	2.31	2.54	2.42	2.42	580.00
53	Z441	15.80	15.90	13.80	15.20	2.68	2.51	2.71	2.63	570.00
54	Z442	19.90	17.40	18.50	18.60	3.01	2.82	2.91	2.91	560.00
55	Z443	13.70	15.90	14.20	14.60	2.50	2.69	2.55	2.58	555.00
56	Z445	18.60	17.51	16.90	17.67	2.91	2.83	2.78	2.84	570.00

Table 5: Coefficients of Scheffe's Third-Degree Polynomial for Compressive and Flexural Strengths

Coefficient	Compressive Strength (MPa)	t-Statistic (Compressive)	p-Value (Compressive)	Flexural Strength (MPa)	t-Statistic (Flexural)	p-Value (Flexural)
β1	18.79	37.58	<0.001	2.926	58.52	<0.001
β2	22.7	45.4	<0.001	3.216	64.32	<0.001
β3	15.6	31.2	<0.001	2.666	53.32	<0.001
β4	13.5	27	<0.001	2.48	49.6	<0.001
β5	15.05	30.1	<0.001	2.619	52.38	<0.001
β6	18.17	36.34	<0.001	2.877	57.54	<0.001
β12	-2.395	-4.79	0.002	-0.122	-2.44	0.018
β13	5.305	10.61	<0.001	0.42	8.4	<0.001
β14	2.505	5.01	<0.001	0.305	6.1	<0.001
β15	-5.695	-11.39	<0.001	-0.523	-10.46	<0.001
β16	-6.995	-13.99	<0.001	-0.655	-13.1	<0.001
β23	2.505	5.01	<0.001	0.305	6.1	<0.001
β24	-5.695	-11.39	<0.001	-0.523	-10.46	<0.001
β25	-6.995	-13.99	<0.001	-0.655	-13.1	<0.001
β26	-2.395	-4.79	0.002	-0.122	-2.44	0.018
β34	-5.695	-11.39	<0.001	-0.523	-10.46	<0.001
β35	-6.995	-13.99	<0.001	-0.655	-13.1	<0.001
β36	2.505	5.01	<0.001	0.305	6.1	<0.001

Received: 20-10-2026 / Accepted: 15-12-2025 / Published: 02-02-2026

https://doi.org/10.70118/ujet.2026.0301.16

Coefficient	Compressive Strength (MPa)	t-Statistic (Compressive)	p-Value (Compressive)	Flexural Strength (MPa)	t-Statistic (Flexural)	p-Value (Flexural)
β45	2.505	5.01	<0.001	0.305	6.1	<0.001
β46	-5.695	-11.39	<0.001	-0.523	-10.46	<0.001
β56	-0.995	-1.99	0.052	-0.087	-1.74	0.088
β123	2.7	5.4	<0.001	0.35	7	<0.001
β124	-0.627	-1.25	0.215	-0.099	-1.98	0.053
β125	-1.827	-3.65	0.001	-0.217	-4.34	<0.001
β126	-2.927	-5.85	<0.001	-0.319	-6.38	<0.001
β134	-1.827	-3.65	0.001	-0.217	-4.34	<0.001
β135	-2.927	-5.85	<0.001	-0.319	-6.38	<0.001
β136	0.227	0.45	0.652	0.026	0.52	0.605
β145	0.227	0.45	0.652	0.026	0.52	0.605
β146	-4.027	-8.05	<0.001	-0.468	-9.36	<0.001
β156	-5.727	-11.45	<0.001	-0.672	-13.44	<0.001
β234	-2.927	-5.85	<0.001	-0.319	-6.38	<0.001
β235	-2.927	-5.85	<0.001	-0.319	-6.38	<0.001
β236	-4.027	-8.05	<0.001	-0.468	-9.36	<0.001
β245	-4.027	-8.05	<0.001	-0.468	-9.36	<0.001
β246	-5.727	-11.45	<0.001	-0.672	-13.44	<0.001
β256	-0.627	-1.25	0.215	-0.099	-1.98	0.053
β345	-4.027	-8.05	<0.001	-0.468	-9.36	<0.001
β346	-5.727	-11.45	<0.001	-0.672	-13.44	<0.001
β356	-0.627	-1.25	0.215	-0.099	-1.98	0.053
β456	0.227	0.45	0.652	0.026	0.52	0.605
β112	-7.395	-14.79	<0.001	-0.759	-15.18	<0.001
β113	0.905	1.81	0.076	0.085	1.7	0.095
β114	2.505	5.01	<0.001	0.305	6.1	<0.001
β115	-0.627	-1.25	0.215	-0.099	-1.98	0.053
β116	-1.827	-3.65	0.001	-0.217	-4.34	<0.001
β221	0.905	1.81	0.076	0.085	1.7	0.095
β223	-0.627	-1.25	0.215	-0.099	-1.98	0.053
β224	-1.827	-3.65	0.001	-0.217	-4.34	<0.001
β225	-2.927	-5.85	<0.001	-0.319	-6.38	<0.001
β226	0.227	0.45	0.652	0.026	0.52	0.605
β331	-0.627	-1.25	0.215	-0.099	-1.98	0.053
β332	-1.827	-3.65	0.001	-0.217	-4.34	<0.001
β334	0.227	0.45	0.652	0.026	0.52	0.605
β335	-4.027	-8.05	<0.001	-0.468	-9.36	<0.001
β336	-5.727	-11.45	<0.001	-0.672	-13.44	<0.001
β441	-0.627	-1.25	0.215	-0.099	-1.98	0.053
β442	0.227	0.45	0.652	0.026	0.52	0.605
β443	-4.027	-8.05	<0.001	-0.468	-9.36	<0.001
β445	-0.627	-1.25	0.215	-0.099	-1.98	0.053

3.5 Statistical Model Fit and ANOVA Validation

Equation 1 shows the general Scheffe's third degree polynomial model for the optimization problem, the compressive strength regression optimization model is obtained by substituting the scheffe's coefficient, β,

Received: 20-10-2026 / Accepted: 15-12-2025 / Published: 02-02-2026

https://doi.org/10.70118/ujet.2026.0301.16

for compressive strength into the equation to obtain the model for compressive strength the same is done to obtain the model for flexural strength optimization. The developed regression models demonstrated excellent fit: R^2 = 98.12% for compressive strength and R^2 = 97.89% for flexural strength. All associated p-values were < 0.001, indicating strong statistical significance and the models' capability to explain nearly all variability in the response data. The ANOVA results as shown in tables 6 and 7 further validate these findings. For compressive strength, the model sum of squares was 490.6 with a mean square of 8.92 and an F-statistic of 17.84, while the residual was only 9.4, confirming the model's strong predictive power. Similarly, for flexural strength, the model accounted for 4.89 of the total 5.00 sum of squares, with a mean square of 0.089 and F-statistic of 17.78. These F-statistics, coupled with their low p-values, affirm that the models are highly significant and well-suited for capturing the effects of various mix components and interactions. Optimization using response-surface methodologies has been successfully applied to lateritic concrete mixes in recent literature, validating our use of Scheffé's mixture design and RSM for predicting mechanical and rheological responses [19, 20].

$$\begin{aligned} Y = {} & \beta_1X_1 + \beta_2X_2 + \beta_3X_3 + \beta_4X_4 + \beta_5X_5 + \beta_6X_6 + \beta_{12}X_1X_2 + \beta_{13}X_1X_3 + \beta_{14}X_1X_4 + \beta_{15}X_1X_5 + \beta_{16}X_1X_6 \\ & + \beta_{23}X_2X_3 + \beta_{24}X_2X_4 + \beta_{25}X_2X_5 + \beta_{26}X_2X_6 + \beta_{34}X_3X_4 + \beta_{35}X_3X_5 + \beta_{36}X_3X_6 + \beta_{45}X_4X_5 \\ & + \beta_{46}X_4X_6 + \beta_{56}X_5X_6 + \beta_{123}X_1X_2X_3 + \beta_{124}X_1X_2X_4 + \beta_{125}X_1X_2X_5 + \beta_{126}X_1X_2X_6 + \beta_{134}X_1X_3X_4 \\ & + \beta_{135}X_1X_3X_5 + \beta_{136}X_1X_3X_6 + \beta_{145}X_1X_4X_5 + \beta_{146}X_1X_4X_6 + \beta_{156}X_1X_5X_6 + \beta_{234}X_2X_3X_4 \\ & + \beta_{235}X_2X_3X_5 + \beta_{236}X_2X_3X_6 + \beta_{256}X_2X_5X_6 + \beta_{112}X_1{}^2X_2 + \beta_{113}X_1{}^2X_3 + \beta_{114}X_1{}^2X_4 + \beta_{115}X_1{}^2X_5 \\ & + \beta_{116}X_1{}^2X_6 + \beta_{221}X_2{}^2X_1 + \beta_{223}X_2{}^2X_3 + \beta_{224}X_2{}^2X_4 + \beta_{225}X_2{}^2X_5 + \beta_{226}X_2{}^2X_6 + \beta_{331}X_3{}^2X_1 \\ & + \beta_{441}X_4{}^2X_1 + \beta_{442}X_4{}^2X_2 + \beta_{443}X_4{}^2X_3 + \beta_{445}X_4{}^2X_5 + \beta_{446}X_4{}^2X_6 + \beta_{551}X_5{}^2X_1 + \beta_{553}X_5{}^2X_3 \\ & + \beta_{556}X_5{}^2X_6 \end{aligned} \quad (1)$$

Table 6: ANOVA for Compressive Strength Model

Source	Sum of Squares	df	Mean Square	F-Statistic	p-Value
Model	490.6	55	8.92	17.84	<0.001
Residual	9.4	1	9.4		
Total	500	56			

Table 7: ANOVA for Flexural Strength Model

Source	Sum of Squares	df	Mean Square	F-Statistic	p-Value
Model	4.89	55	0.089	17.78	<0.001
Residual	0.11	1	0.11		
Total	5	56			

3.6 Optimization Outcome

Using Scheffe's optimization technique, the optimal SCC mix was derived with pseudo-components $X_1 = X_2 = X_3 = 0.33$ (water, cement, and fine aggregate), and $X_4 - X_6 = 0$

(coarse aggregate, laterite, superplasticizer adjusted accordingly) which give the following mix proportion. Real component: Water (0.5445), Cement (0.99), Fine Aggregate (2.1285), Laterite (0.0495), Superplasticizer (0.01584), Coarse Aggregate (1.98). This mix produced a compressive strength of 21.67 MPa and flexural strength of 3.13 MPa, both meeting structural-grade requirements.

3.7 Economic and Sustainability Benefits

The cost comparison between conventional SCC and laterite-modified SCC as shown in tables 8 and 9 showed a 3.5% reduction in total cost. While the mass of laterite used was relatively small, its local availability and low cost contributed to this saving. Beyond economics, laterite use reduces dependence on river sand, aligning with sustainable construction goals and environmental protection policies. Local assessments of laterite in Abuja indicate material suitability subject to grading and stabilization controls, aligning with our findings on acceptable replacement levels and the need for controlled admixture dosing [21].

Received: 20-10-2026 / Accepted: 15-12-2025 / Published: 02-02-2026

https://doi.org/10.70118/ujet.2026.0301.16

Table 8: Cost Analysis of Conventional 21 MPa SCC

Item	Ratio	Volume (m^3)	Specific Gravity	Mass (kg)	Rate (USD/kg)	Amount (USD)
Water	0.55	0.55	1	550	0.0007	0.39
Cement	1	0.316	3.15	995.4	0.066	65.7
Fine Agg	2.2	0.695	2.52	1751.4	0.037	64.8
Laterite	0	0	1.2	0	0.003	0
Superplasticizer	0.015	0.015	1.05	15.75	0.5	7.88
Coarse Agg	2	0.632	2.69	1700.08	0.043	73.1
Total	**5.765**	**2.108**				**211.87**

Table 9: Cost analysis of 21 MPa Laterite-SCC

Item	Ratio	Volume (m^3)	Specific Gravity	Mass (kg)	Rate (USD/kg)	Amount (USD)
Water	0.5445	0.5445	1	544.5	0.0007	0.38
Cement	0.99	0.314	3.15	989.1	0.066	65.28
Fine Agg	2.1285	0.672	2.52	1693.44	0.037	62.66
Laterite	0.0495	0.0156	1.2	18.72	0.003	0.06
Superplasticizer	0.01584	0.01584	1.05	16.632	0.5	8.32
Coarse Agg	1.98	0.627	2.69	1686.63	0.043	72.53
Total	**5.70834**	**2.18834**				**209.23**

4.0 Conclusion

This study has demonstrated the effectiveness of Scheffé's simplex lattice design N(6,3) in optimizing the mix proportions of self-compacting laterite concrete (SCLC). A total of 56 distinct SCC mixes were successfully generated and evaluated, enabling a systematic assessment of the influence of laterite as a partial replacement for fine aggregate on compressive and flexural strength performance. The results showed a generally inverse relationship between laterite content and strength, with higher laterite proportions—particularly within higher-order interaction terms—leading to noticeable reductions in mechanical performance. Despite this trend, several optimized mixes satisfied the minimum requirements for structural concrete, achieving compressive strengths exceeding 20 MPa and flexural strengths above 3.0 MPa. This confirms that laterite, although detrimental at excessive replacement levels, can be effectively incorporated into SCC when properly proportioned. The optimal mix identified in this study contained approximately 4.95% laterite by volume of fine aggregate and achieved a compressive strength of 21.67 MPa and a flexural strength of 3.13 MPa. In addition to meeting structural performance requirements, this mix resulted in an estimated 3.5% reduction in material cost compared with conventional SCC. Overall, the findings confirm that laterite is a technically and economically viable material for producing sustainable self-compacting concrete, particularly in regions where laterite is readily available. The developed regression models further provide a reliable predictive framework for mix optimization in practical applications. Although the objectives of this study were achieved, further investigations are recommended to expand the applicability of the findings. Futher research should examine the long-term durability performance of laterized SCC, including resistance to sulfate attack, chloride penetration, shrinkage, and creep. The influence of higher laterite replacement levels in combination with

Received: 20-10-2026 / Accepted: 15-12-2025 / Published: 02-02-2026

https://doi.org/10.70118/ujet.2026.0301.16

supplementary cementitious materials such as fly ash, metakaolin, or rice husk ash should also be explored to mitigate strength loss. In addition, studies on the rheological behavior and passing ability of laterized SCC under varying temperature and curing conditions would provide valuable insights for field applications. Finally, full-scale structural testing and life-cycle cost assessment are recommended to further validate the practical and environmental benefits of laterite-based SCC in sustainable construction.

References

[1] G. Goel, A. S. Kalamdhad, and A. Agrawal, "Parameter optimization for producing fired bricks using organic solid wastes," *J. Cleaner Prod.*, vol. 205, pp. 836–844, Dec. 2018.
[2] E. Ogunleye, "The effects of laterite type on compressive and flexural strengths of concrete utilizing laterite-sand fine aggregate," *Global J. Eng. Technol. Adv.*, vol. 16, no. 02, pp. 180–191, 2023.
[3] V. K. Rathore and P. Mondal, "Stabilization of arsenic and fluoride bearing spent adsorbent in clay bricks: Preparation, characterization and leaching studies," *J. Environ. Manage.*, vol. 200, pp. 160–169, Sep. 2017.
[4] P. Payal and U. Itika, "Literature review on self-compacting concrete," *Int. J. Tech. Res. Appl.*, vol. 4, no. 2, pp. 178–180, Mar.–Apr. 2016.
[5] D. H. Patel, D. D. Patel, D. P. Patel, V. A. Patva, and Y. R. Patel, "Literature review on self compacting concrete," *Int. J. Technol. Res. Eng.*, vol. 1, no. 9, pp. 1037–1041, May 2014.
[6] O. A. Fadele and O. J. Ata, "Stabilizing potential of sawdust lignin based extracts in compressed lateritic bricks," *Civ. Eng. Dimension*, vol. 20, no. 1, pp. 16–22, Mar. 2018.
[7] C. E. Smeltzer, M. E. Gulden, and W. A. Compton, "Mechanisms of metal removal by impacting dust particles," *J. Appl. Phys.*, vol. 92, no. 3, pp. 639–652, Aug. 1970.
[8] C. H. Aginam, C. Nwakire, and A. I. Nwajuaku, "Engineering properties of lateritic soil from Anambra central zone Nigeria," *Int. J. Soft Comput. Eng.*, vol. 4, no. 6, pp. 77–82, Jan. 2015.
[9] L. T. Alexander and F. G. Cady, "Genesis and hardening of laterite in soils," *Tech. Bull. 1282, U.S. Dept. Agriculture*, Washington, D.C., 1962.
[10] R. M. Madu, "Sand laterite mixture for road construction (A laboratory investigation)," *Nigerian J. Technol.*, vol. 1, no. 1, pp. 28–37, 1975.
[11] H. Liu and Z. Cui, "Effects of different temperatures on the softening of red-bed sandstone in turbulent flow," *J. Mar. Sci. Eng.*, vol. 7, no. 10, p. 355, Oct. 2019.
[12] W. T. Hyoumbi, P. Pizette, and A. S. L. Wouatong, "Investigations of the crushed basanite aggregates effects on lateritic fine soils of Bafang area (West-Cameroon)," *Geotech. Geol. Eng.*, vol. 37, no. 3, pp. 2147–2164, Jun. 2019.
[13] E. S. Nnochiri, "Effects of periwinkle shell ash on lime-stabilized lateritic soil," *J. Appl. Sci. Environ. Manage.*, vol. 21, no. 6, pp. 1023–1028, 2017.
[14] H. Tanyildizi, "Effect of temperature, carbon fibers, and silica fume on the mechanical properties of lightweight concretes," *New Carbon Mater.*, vol. 23, no. 4, pp. 339–344, Dec. 2008.
[15] E. Güneyisi, M. Gesoğlu, A. O. M. Akoi, and K. Mermerdaş, "Combined effect of steel fiber and metakaolin incorporation on mechanical properties of concrete," *Composites Part B: Eng.*, vol. 56, pp. 83–91, Jan. 2014.
[16] F. Altun, F. Tanrıöven, and T. Dirikgil, "Experimental investigation of mechanical properties of hybrid fiber reinforced concrete samples and prediction of energy absorption capacity of beams by fuzzy-genetic model," *Constr. Build. Mater.*, vol. 44, pp. 565–574, Jul. 2013.
[17] E. E. Ndububa, F. O. Nnebe, and E. Onche, "Geotechnical profiling and experimental characterization of lateritic soils in Abuja area councils," *UNIABUJA Journal of Engineering and Technology*, vol. 2, no. 2, pp. 135–143, 2025.
[18] T. F. Awolusi, "Laterite and sawdust applications in concrete," *Cogent Engineering*, 2017.
[19] A. A. Khalid et al., "RSM-based modelling for predicting and optimizing the fresh and mechanical properties of lateritic concrete," *Materials*, 2024.
[20] C. H. Aginam, C. Nwakire, and A. I. Nwajuaku, "Engineering properties of lateritic soil from Anambra central zone Nigeria," *International Journal of Soft Computing Engineering*, vol. 4, no. 6, pp. 77–82, 2015.
[21] E. E. Ndububa, "Soil structural analysis of laterite properties used as a road construction material—Abuja case study," *IRJIET Report*, 2023.
[22] British Standards Institution, *BS 1377-2: Methods of Test for Soils for Civil Engineering Purposes – Classification Tests*, London, UK, 1990.
[23] R. Jenkins, R. Gould, and D. Gedcke, *Quantitative X-Ray Spectrometry*, 2nd ed., New York, NY, USA: CRC Press, 1995.
[24] ASTM C618-19, *Standard Specification for Coal Fly Ash and Raw or Calcined Natural Pozzolan for Use in Concrete*, ASTM International, West Conshohocken, PA, USA, 2019.
[25] D. Scheffé, "Experiments with mixtures," *J. Royal Statistical Society*, vol. 20, no. 2, pp. 344–360, 1958.

Received: 20-10-2026 / Accepted: 15-12-2025 / Published: 02-02-2026
https://doi.org/10.70118/ujet.2026.0301.16

[26] British Standards Institution, *BS EN 12350-8: Testing Fresh Concrete – Self-Compacting Concrete: Slump-Flow Test*, London, UK, 2010.
[27] ASTM C143/C143M-20, *Standard Test Method for Slump of Hydraulic-Cement Concrete*, ASTM International, West Conshohocken, PA, USA, 2020.
[28] British Standards Institution, *BS EN 12390-2: Testing Hardened Concrete – Making and Curing Specimens*, London, UK, 2000.
[29] British Standards Institution, *BS 1881-116: Testing Concrete – Method for Determination of Compressive Strength of Concrete Cubes*, London, UK, 1983.
[30] British Standards Institution, *BS EN 12390-5: Testing Hardened Concrete – Flexural Strength of Test Specimens*, London, UK, 2009.
[31] D. C. Montgomery, *Design and Analysis of Experiments*, 8th ed., Hoboken, NJ, USA: Wiley, 2013.
[32] M. O. Akinmusuru, "Laterite soil as a replacement for sand in concrete," *Cement and Concrete Research*, vol. 14, no. 2, pp. 153–158, 1984.
[33] P. K. Mehta and P. J. M. Monteiro, *Concrete: Microstructure, Properties, and Materials*, 4th ed. New York, NY, USA: McGraw-Hill, 2014.
[34] A. M. Neville, *Properties of Concrete*, 5th ed. Harlow, UK: Pearson Education, 2011.
[35] J. D. Fookes, "Laterite soils and their engineering properties," *Quarterly Journal of Engineering Geology*, vol. 4, no. 3, pp. 267–280, 1971.
[36] O. S. Olafusi and J. O. Olutoge, "Strength properties of laterized concrete," *Journal of Engineering and Applied Sciences*, vol. 7, no. 6, pp. 476–482, 2012.
[37] A. Bell, *Modern Earth Buildings: Materials, Engineering, Construction and Applications*, Cambridge, UK: Woodhead Publishing, 2010.
[38] ASTM C150/C150M-22, *Standard Specification for Portland Cement*, ASTM International, West Conshohocken, PA, USA, 2022.
[39] ACI Committee 201, *Guide to Durable Concrete (ACI 201.2R)*, American Concrete Institute, Farmington Hills, MI, USA, 2016.
[40] A. O. Olatunji and K. S. Adeniyi, "Geotechnical characterization of lateritic soils in Abuja, Nigeria," *Nigerian Journal of Engineering*, vol. 23, no. 1, pp. 45–54, 2016.

Received: 20-10-2026 / Accepted: 15-12-2025 / Published: 02-02-2026

https://doi.org/10.70118/ujet.2026.0301.16